# Store-independent coupling between the Secretory Pathway $Ca^{2+}$ transport ATPase SPCA1 and Orai1 in Golgi stress and Hailey-Hailey disease

Susanne Smaardijk[1], Jialin Chen[1], Sara Kerselaers[2,3], Thomas Voets[2,3], Jan Eggermont[1], Peter Vangheluwe[1,*]

**Affiliations**
From the [1]Laboratory of Cellular Transport Systems; [2]Laboratory of Ion Channel Research, Department of Cellular and Molecular Medicine, KU Leuven Belgium; [3]VIB Center for Brain & Disease Research, Leuven, Belgium

**To whom correspondence should be addressed:**

Prof. Peter Vangheluwe, Laboratory of Cellular Transport Systems, Department of Cellular and Molecular Medicine, ON1 Campus Gasthuisberg, KU Leuven, Herestraat 49/box 802, 3000 Leuven, Belgium;
Telephone: +32 16 330720
Email: peter.vangheluwe@kuleuven.be

**Key words:** Golgi stress response, calcium transport, store operated $Ca^{2+}$ entry, breast cancer, organelle contact site

1

[1] **Abbreviations:** ER: Endoplasmic reticulum; GASE: Golgi Apparatus stress recognition element; HHD: Hailey-Hailey Disease; KD: knockdown; NFAT: Nuclear factor of activated T cells; NT: non-targeting; ROI: Region of interest; SICE: Store-independent $Ca^{2+}$ entry; SOCE: Store-operated $Ca^{2+}$ entry; SPCA: Secretory pathway $Ca^{2+}$ ATPase; STIM1: Stromal interaction molecule 1; TFE3: Transcription factor E3; TG: Thapsigargin; TGN: *trans*-Golgi network; Xyloside: 4-methylumbelliferyl-β-D-xylopyranoside

**Abstract**

The secretory pathway $Ca^{2+}$ ATPases SPCA1 and SPCA2 transport $Ca^{2+}$ and $Mn^{2+}$ into the Golgi and secretory pathway. SPCA2 mediates store-independent $Ca^{2+}$ entry (SICE) via STIM1-independent activation of Orai1, inducing constitutive $Ca^{2+}$ influx in mammary epithelial cells during lactation. Here, we show that like SPCA2, also the overexpression of the ubiquitous SPCA1 induces cytosolic $Ca^{2+}$ influx, which is abolished by Orai1 knockdown and occurs independently of STIM1. This process elevates the $Ca^{2+}$ concentration in the cytosol and in the non-endoplasmic reticulum (ER) stores, pointing to a functional coupling between Orai1 and SPCA1. In agreement with this, we demonstrate via Total Internal Reflection Fluorescence microscopy that Orai1 and SPCA1a co-localize near the plasma membrane. Interestingly, SPCA1 overexpression also induces Golgi swelling, which coincides with translocation of the transcription factor TFE3 to the nucleus, a marker of Golgi stress. The induction of Golgi stress depends on a combination of SPCA1 activity and SICE, suggesting a role for the increased $Ca^{2+}$ level in the non-ER stores. Finally, we tested whether impaired SPCA1a/Orai1 coupling may be implicated in the skin disorder Hailey-Hailey disease (HHD), which is caused by SPCA1 loss-of-function. We identified HHD-associated SPCA1a mutations that impair either the $Ca^{2+}$ transport function, Orai1 activation, or both, while all mutations affect the $Ca^{2+}$ content of the non-ER stores. Thus, the functional coupling between SPCA1 and Orai1 increases cytosolic and intraluminal $Ca^{2+}$ levels, representing a novel mechanism of SICE that may be affected in HHD.

## 1. Introduction

Intracellular $Ca^{2+}$ regulates many cellular processes, and consequently, local $Ca^{2+}$ concentrations in the cytosol and the organelles are usually kept within a narrow physiological window. $Ca^{2+}$ levels in the Golgi and secretory pathway are regulated by the ubiquitous $Ca^{2+}/Mn^{2+}$ transporter SPCA1 (Secretory Pathway $Ca^{2+}/Mn^{2+}$ ATPase isoform 1), a P-type ATPase that undergoes autophosphorylation during transport. In the Golgi apparatus, $Ca^{2+}$ and $Mn^{2+}$ are required for enzymes that exert post-translational modifications, particularly glycosylation [1-3]. In addition, the Golgi $Ca^{2+}$ concentration also regulates Cab45-mediated sorting of proteins for secretion [4]. Four splice variants of SPCA1 (SPCA1a-d) have been described, which differ in their C-terminus [5]. The tissue distribution and functional role of these splice variants remain unclear.

The crucial role for $Ca^{2+}$ and/or $Mn^{2+}$ in Golgi homeostasis is illustrated by disease-causing heterozygous mutations in *ATP2C1*, the gene encoding SPCA1, which evoke Hailey-Hailey disease (HHD, OMIM: 169600) [6]. HHD is a skin disorder that is marked by a disturbed epidermal $Ca^{2+}$ gradient in keratinocytes, which manifests as rashes and blistering of the skin due to acantholysis (loss of cell-to-cell contact). To date, 177 HHD mutations in *ATP2C1* have been identified, but few have been functionally characterized [7]. Many HHD mutations result in a pre-terminal protein truncation, which likely leads to loss of SPCA1 function and haplo-insufficiency [8]. Complete loss of SPCA1 in *ATP2C1*$^{-/-}$ mice leads to premature death due to a failure of neural tube closing [9]. At the cellular level, swelling and fragmentation of the Golgi is observed, which eventually leads to cell death, indicating that a deficit of $Ca^{2+}$ in the Golgi causes Golgi stress [9].

Organelle stress responses are emerging as important feedback mechanisms that maintain or restore cellular homeostasis, or that induce controlled cell death when stress is persistent. Endoplasmic reticulum (ER) stress is by far the best understood organelle stress response, but with the identification of mitochondrial, lysosomal and Golgi stress pathways, a more general concept of organelle homeostasis is emerging. Typically, organelle stress responses depend on sensor proteins that act on downstream signaling pathways, eventually leading to the transcription of a specific set of (often organelle-specific) genes [10]. The sensing proteins for Golgi stress are not yet identified, but some downstream transcription factors (CREB3 and TFE3) and effector proteins (ARF4 and Hsp47) have been described [11]. Transcription factor E3 (TFE3) was first described as a transcription factor for starvation and lysosomal biogenesis, [12], but recently it was found that through an unknown mechanism, TFE3 is dephosphorylated and translocates to the nucleus in conditions of Golgi stress [13]. There it binds

the Golgi apparatus stress response element (GASE), which controls expression of a number of Golgi-related genes [14].

The luminal $Ca^{2+}$ concentration of the ER is regulated by store-operated $Ca^{2+}$ entry (SOCE), which depends on activation of the plasma membrane $Ca^{2+}$ channel Orai1 by Stromal Interaction Molecule 1 (STIM1). Independently of STIM1, the second isoform of the Secretory Pathway $Ca^{2+}/Mn^{2+}$ transport ATPase, SPCA2, is capable of activating Orai1 through a direct interaction [15]. This process is named store-independent $Ca^{2+}$ entry (SICE), since it is activated independently of the ER $Ca^{2+}$ levels. The resulting cytosolic $Ca^{2+}$ rise induces the nuclear translocation of the nuclear factor of activated T-cells (NFAT) [15]. It also increases the $Ca^{2+}$ concentration in thapsigargin (TG)-insensitive stores, which include the Golgi, further demonstrating the store independent role of Orai1 [16]. SICE promotes the cellular uptake of $Ca^{2+}$ in mammary epithelial cells during lactation for subsequent $Ca^{2+}$ delivery to the milk, and may be chronically activated in some forms of breast cancer [15]. In contrast to SPCA2, SPCA1 overexpression does not promote NFAT translocation [15, 16], suggesting that SPCA1 may not be capable of activating Orai1. However, a C-terminal fragment of SPCA1a elicits NFAT translocation [15], which suggests that also SPCA1 contains elements for Orai1 activation.

Here, we describe the activation of Orai1 by SPCA1a, which, similar to SPCA2, leads to constitutive $Ca^{2+}$ influx and subsequent $Ca^{2+}$ transfer into intracellular compartments. We further explore the possibility that the SPCA1a/Orai1 interaction is implicated in the Golgi stress response and/or HHD.

## 2. Materials and methods

### *2.1 Constructs, cell culture and transfection*

Human SPCA1a, SPCA1b, SPCA1d and SPCA2 cDNA were inserted into pcDNA6 destination vectors (Gateway, Thermo Fisher Scientific) with an N-terminal mCherry-tag. Mutants were generated using the Quickchange site-directed mutagenesis kit (Stratagene) or the Q5 site-directed mutagenesis kit (Bioké). The TFE3-GFP construct was a kind gift from Dr. H. Yoshida, Japan [13]. The Orai1-GFP construct was provided by Dr. M. Hediger, Institute of Biochemistry and Molecular Medicine, Switzerland. HEK293T cells were cultured at 37 $^{\circ}$C and 10% $CO_2$, while HeLaT1 cells were cultured at 37 $^{\circ}$C and 5% $CO_2$. Cells were cultured in Dulbecco's Modified Eagle Medium supplemented with 10% fetal bovine serum, 100 IU/ml penicillin, 100 mg/ml streptomycin and 2 mM Glutamax (Thermo Fisher Scientific). GeneJuice transfection reagent (Thermo Fisher Scientific) was used for transfection according to the manufacturer's instructions. Co-transfection of plasmid DNA and siRNA

oligonucleotides (OnTarget Plus, Dharmacon) was achieved with Dharmafect Duo (GE Life Science) according to the manufacturer's protocol.

*2.2 Fluorescence imaging*

Cells were seeded at 7,500 cells/well in a four-chamber glass-bottom dish (Cellvis) and transfected with 75 ng TFE3-GFP plasmid DNA and 100 ng mCherry-tagged SPCA1a/2 plasmid DNA. 72 h after transfection, cells were fixed in 4% paraformaldehyde (Sigma-Aldrich), and 100 cells were counted per condition to determine the percentage of cells with nuclear TFE3 translocation. For *trans*-Golgi network (TGN) staining, cells were fixed with 4% paraformaldehyde, permeabilized with 0.1% Triton X-100, blocked for 1 h with 1% BSA in PBS and incubated for 1 h with anti-TGN46 (Thermo Scientific, 1:500) and 1 h with Alexa Fluo 488 anti-rabbit (Fischer Scientific, 1:2000) in 3% BSA in PBS. The nuclei were stained with DAPI (1 µg/ml, 30 min). Visualization was performed on an Olympus IX81 fluorescence microscope.

*2.3 Determination of Golgi size*

The size of the Golgi was determined relative to the size of the nucleus. Cells with approximately equal protein expression were selected. With ImageJ quantification software, each cell was marked as a region of interest (ROI), and the image was split into red, green and blue color channels. The total intensity of the green channel (TGN46) was compared to the blue channel (DAPI) for each ROI. The TGN/DAPI area ratio was used as a readout for the Golgi size relative to the nucleus.

*2.4 Fura2-AM $Ca^{2+}$ measurements*

HEK293T cells were transfected with mCherry-tagged constructs. 72 h after transfection, cells were incubated for 30 min in a modified KREBS solution (135 mM NaCl, 6.2 mM KCl, 1.2 mM $MgCl_2$, 12 mM HEPES, pH 7.3, 11.5 mM glucose and 1.5 mM $CaCl_2$) supplemented with 1 µM Fura2-AM (Life Sciences), and washed for 30 min in KREBS solution. Ten mCherry-positive cells were selected and visualized on a Zeiss Axio Observer Z1 Inverted Microscope. Extracellular $Ca^{2+}$ was depleted by adding calcium-free KREBS supplemented with 3 mM BAPTA (Alfa Aesar) to the cells. $Ca^{2+}$ release from ER and non-ER stores was assessed by adding respectively 500 nM thapsigargin (Alomone Labs) or 2 µM ionomycin (Enzo Life Sciences) in calcium-free KREBS supplemented with 3 mM BAPTA. SOCE was induced by adding 500 nM thapsigargin in calcium-free KREBS supplemented with 3 mM BAPTA, followed by KREBS solution with $Ca^{2+}$.

*2.5 Total Internal Reflection Fluorescence (TIRF) microscopy*

TIRF microscopy was performed on HEK293T cells overexpressing SPCA1a or SPCA2 and Orai1 using an inverted Zeiss Axio Observer.Z1 microscope with a 100x oil objective (numerical aperture = 1.45), 488-nm and 561-nm lasers and a Hamamatsu Orca-R2 CCD camera, as described in [17]. Experiments were performed in the same modified KREBS solution as the Fura2-AM $Ca^{2+}$ measurements. The TIRF angle was chosen such that the evanescent wave decayed with a length constant of 120 nm.

*2.6 ATPase assay*

$Ca^{2+}$-dependent ATPase activity measurements of SPCA1a WT and mutants were performed on microsomes of HEK293T cells as described earlier [18]. 2 µg protein per well was used for WT SPCA1a, whereas for the mutants the amount of protein was adjusted based on the relative expression levels on an immunoblot to reach equal SPCA1a levels in the assay.

*2.7 Statistics*

Origin 8.6 was used for data analysis. Results are represented as average ± SEM, unless indicated otherwise. Multiple comparison statistical analysis was carried out by one-way ANOVA followed by a post-hoc Bonferroni test. $P \leq 0.05$ was considered statistically significant.

**3. Results**

*3.1 SPCA1a induces $Ca^{2+}$ influx via Orai1 activation*

Feng *et al.* have shown that SPCA2 interacts with Orai1 to constitutively activate its $Ca^{2+}$ gating function, leading to a higher cytosolic $Ca^{2+}$ concentration and translocation of the transcription factor NFAT to the nucleus [15]. Overexpression of SPCA1a in HEK293T cells does not induce translocation of NFAT [15], which we also confirmed earlier [16]. To follow the $Ca^{2+}$ alterations in the cell during SICE, we used Fura2-AM to measure cytosolic $Ca^{2+}$ levels in HEK293T cells before ($R_0$) and after ($R_{120}$) addition of the extracellular $Ca^{2+}$ chelator BAPTA (Figure 1A). The ratio $R_0/R_{120}$ is an indicator of the $Ca^{2+}$ influx over the plasma membrane. As previously established, cells overexpressing SPCA2 display a considerably higher constitutive $Ca^{2+}$ influx ($R_0/R_{120} = 1.29 \pm 0.04$) than cells transfected with mCherry vector ($R_0/R_{120} = 1.03 \pm 0.01$) (Figure 1B). This confirms that the $Ca^{2+}$ influx over the plasma membrane is low under resting conditions, while overexpression of SPCA2 induces $Ca^{2+}$ influx, which depends on the opening of the endogenous Orai1 channels [15, 16]. In our experimental setting, overexpression of SPCA1a had a similar effect as SPCA2, with an $R_0/R_{120}$ of $1.21 \pm 0.03$. This indicates that SPCA1a can also induce $Ca^{2+}$ influx over the plasma membrane, which unlike SPCA2 does not lead to NFAT translocation [15, 16]. This happens independently of the ability of the transport capacity of the pump,

since mutations in the catalytic autophosphorylation (D350N) and dephosphorylation (E189Q) motifs of SPCA1a do not prevent the induction of SICE (Figure 1B), similar to what was previously found for SPCA2 [15, 16]. SICE is also observed with the other SPCA1 splice variants SPCA1b and SPCA1d (Figure 1C). SPCA1c was not included, since this is a truncated and unstable splice variant that is rapidly degraded. We found that all tested SPCA1 splice variants display a similar SICE response [19]. For all further experiments, we used SPCA1a.

Overexpression of SPCA1a or SPCA2 also increased the $R_0/R_{120}$ in HeLaT1 cells and BEM17 neuroblastoma cells (Figure 1D) indicating that SPCA1a-mediated $Ca^{2+}$ influx takes place in multiple cell types. As the $R_0/R_{120}$ was highest in HEK293T cells, we continued with this cell line for further experiments.

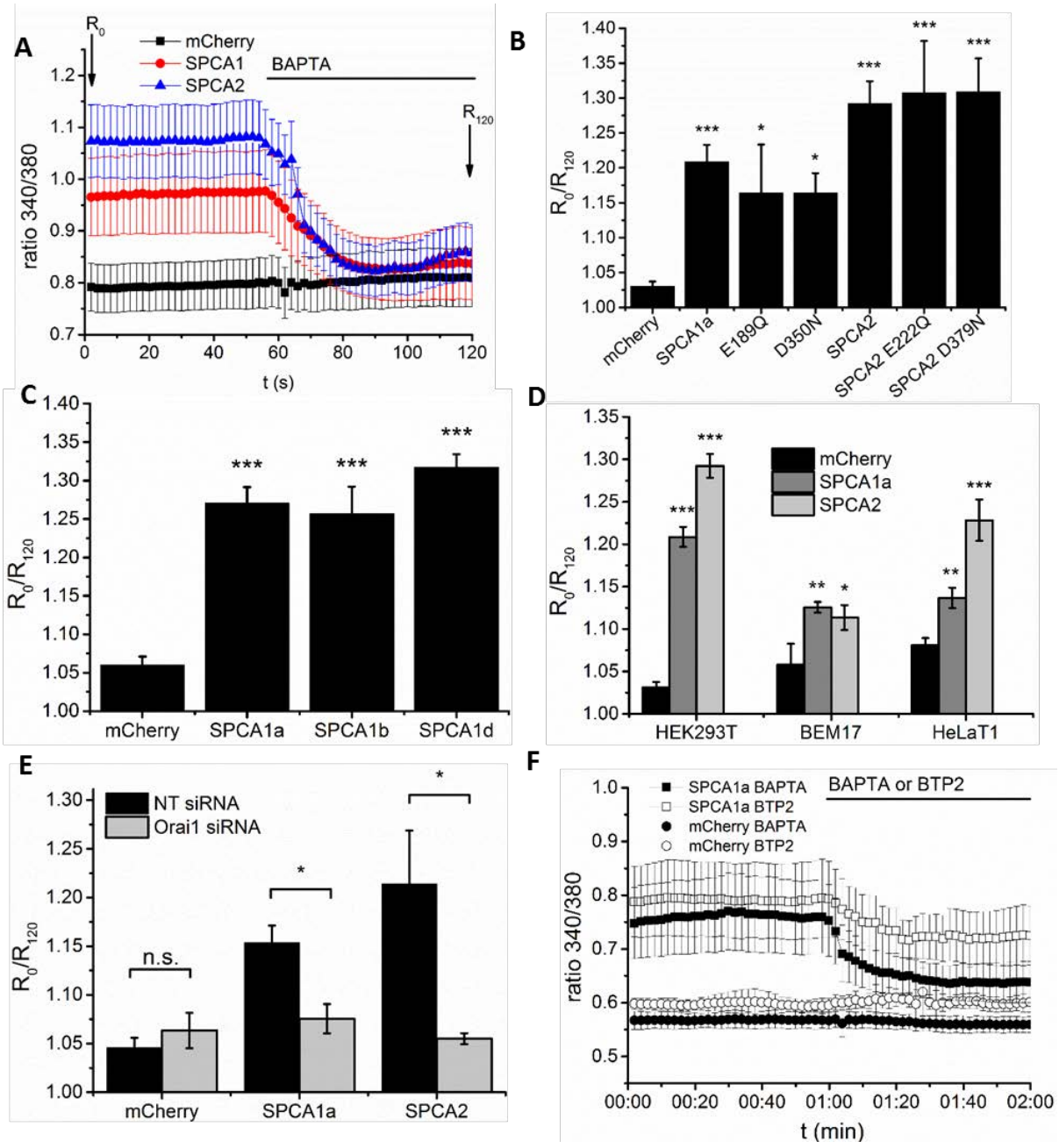


**Figure 1: SPCA1a increases constitutive $Ca^{2+}$ influx in a similar manner as SPCA2**. A) Fura2 traces of $[Ca^{2+}]_{cyt}$ for HEK293T overexpressing mCherry or mCherry-tagged SPCA1a or SPCA2. At the indicated time point, 3 mM BAPTA was added to the cells. B) $R_0/R_{120}$ values (ratio before (0 s) and after addition of BAPTA (120 s)) for HEK293T cells overexpressing SPCA1a or SPCA2 WT or inactive mutants. C) $R_0/R_{120}$ values for the splice variants SPCA1a, SPCA1b and SPCA1d. D) Comparison of $R_0/R_{120}$ values for HEK293T, HeLaT1 and BEM17 cell lines overexpressing SPCA1a or SPCA2 WT. E) $R_0/R_{120}$ values for cells overexpressing mCherry or SPCA isoforms in combination with knockdown of Orai1. F) Addition of the CRAC-channel inhibitor BTP2 (open symbols) has a similar effect on $[Ca^{2+}]_{cyt}$ as addition of BAPTA (closed symbols). 10 cells were measured per Fura-2 experiment, n=3-8. Results are depicted as average ± SEM. *:p<0.05; **: p<0.01; ***: p<0.005

Like for SPCA2, the mechanism of SPCA1a-mediated $Ca^{2+}$ influx may depend on Orai1. To confirm this, we measured constitutive $Ca^{2+}$ influx in HEK293T cells where SPCA1a was overexpressed, while Orai1 was knocked down (KD) by siRNA. In Orai1 KD cells, overexpression of SPCA1a or SPCA2 yielded similar

$R_0/R_{120}$ values as mCherry-transfected cells (Figure 1E) indicating that the increased constitutive $Ca^{2+}$ influx is dependent on Orai1. Addition of the CRAC-channel inhibitor BTP-2, although less pronounced, showed a trend similar to the addition of BAPTA to deplete extracellular $Ca^{2+}$ (Figure 1F).

To exclude possible involvement of STIM1 and SOCE, we first checked the cellular localization of STIM1 with overexpression of SPCA1a in HeLaT1 cells (Supplementary Figure 1A). STIM1 does not form punctae under conditions of SPCA1a overexpression, indicating that SOCE is not involved (Supplementary Figure 1A). To further evaluate whether STIM1 is involved, we performed knockdown of STIM1 with siRNA in cells that overexpress mCherry or SPCA1a. Upon knockdown, STIM1 protein levels decreased by 65% compared to cells transfected with control (NT) siRNA (Supplementary Figure 1B), which diminished SOCE in both mCherry- and SPCA1a- transfected cells (Supplementary Figure 1C). However, the SICE response is unaltered when STIM1 is knocked down (Supplementary Figure 1D), showing that SPCA1-mediated activation of Orai1 occurs independently of STIM1.

*3.2 SPCA1a transfers Orai1-mediated $Ca^{2+}$ influx into intracellular $Ca^{2+}$ stores*

We previously demonstrated that SPCA2 and Orai1 operate together to shuttle $Ca^{2+}$ from the extracellular environment into TG-insensitive $Ca^{2+}$ stores [16]. Likewise, overexpression of WT SPCA1a significantly increases the $Ca^{2+}$ content of the TG-insensitive stores, in agreement with an increased $Ca^{2+}$ uptake activity (Figure 2A). Although overexpression of the inactive SPCA1a mutants triggers Orai1 activation, this does not significantly increase the $Ca^{2+}$ content of the TG-insensitive pool compared to mCherry-transfected cells. A slightly higher $Ca^{2+}$ level in the TG-insensitive pool is observed for the inactive mutants (not significant), which can be attributed to endogenous SPCA1 that may transfer the $Ca^{2+}$ that enters the cell. Note that overexpression of the SPCA1 WT or dead mutant presents a lower TG-induced $Ca^{2+}$ release than the mCherry control. However, this occurs irrespective of SPCA1 transport activity (Figure 2A) and without evoking a SOCE response (Supplementary Figure 1). This indicates that SICE may work independently of ER $Ca^{2+}$ and may only affect the TG-insensitive pool. Together, these data show that SPCA1a WT is mechanistically coupled to Orai1, shuttling the incoming $Ca^{2+}$ from the cytosol into an intracellular compartment.

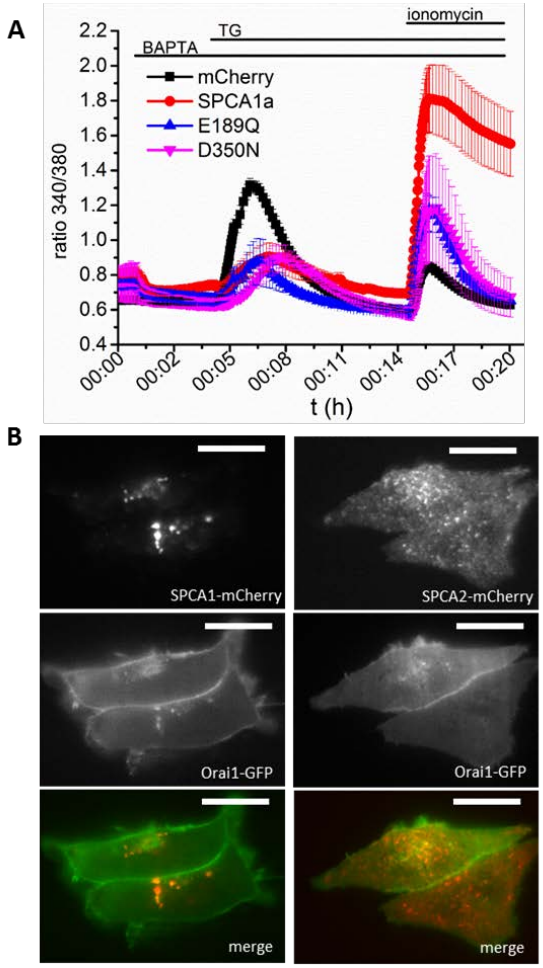


**Figure 2: SPCA1a and Orai1 operate in a microdomain near the plasma membrane to transfer extracellular $Ca^{2+}$ into intracellular stores.** A) Overexpression of SPCA1a results in an increase in $Ca^{2+}$ released from TG-insensitive stores, which is severely diminished when inactive SPCA1a mutants are expressed. B) TIRF microscopy images of HEK293T cells co-transfected with mCherry-tagged SPCA1a or SPCA2 and GFP-tagged Orai1. Scale bar = 10 µm.

To further confirm that Orai1 and SPCA1a may be functionally coupled in a microdomain near the plasma membrane, we used TIRF microscopy, which allows the visualization of the sub-plasma membrane region. In HEK293T cells, GFP-tagged Orai1 displays a clear plasma membrane distribution. mCherry-tagged SPCA1a and SPCA2 present a vesicular pattern in close proximity to the plasma membrane (Figure 2B), which is in line with their presence in the secretory system. Importantly, SPCA1a shows good co-localization with Orai1, whereas the overlap of SPCA2 and Orai1 is less pronounced. We therefore conclude that SPCA1a is in close proximity of Orai1 in a region near the plasma membrane where they may cooperate to transfer extracellular $Ca^{2+}$ into intracellular stores.

*3.3 SPCA1a-mediated $Ca^{2+}$ uptake in intracellular compartments leads to Golgi stress*

We noted that overexpression of SPCA1a significantly increases the size of the Golgi (1.89 ± 0.57-fold as compared to non-transfected cells), which may help to bring SPCA1a closer to the plasma membrane (Figure 3A,B). Moreover, Golgi swelling is a possible sign of Golgi stress [13]. We therefore tested the hypothesis that the SPCA1a/Orai1 activation may play a role in the Golgi stress response. As an additional readout for Golgi stress, we followed the translocation of a GFP-labeled TFE3 transcription factor (TFE3-GFP) into the nucleus (Figure 3C). As positive controls for Golgi stress, we administered the $Na^+/H^+$ ionophore monensin or the sugar analog 4-methylumbelliferyl-β-D-xylopyranoside (xyloside) [11, 14]. After overnight incubation, these compounds resulted in a dose-dependent translocation of TFE3-GFP (Figure 3D,E), as previously reported [14]. We observed TFE3-GFP translocation in 80% of the cells with 0.5 µM monensin or 10 mM xyloside. Incubation with tunicamycin, a trigger of ER stress, did not lead to TFE3-GFP translocation, demonstrating the specificity of the TFE3-GFP response (data not shown).

Importantly, in the absence of monensin or xyloside, the overexpression of WT SPCA1a or SPCA2 alone also induced TFE3-GFP translocation in up to 40% of the HEK293T cells, indicative of mild Golgi stress (Figure 3D,E). Although the catalytic dead mutants D350N (SPCA1a) and D379N (SPCA2) both activate Orai1, the induction of TFE3-GFP translocation is not statistically different from control (Figure 3F). The difference between SPCA1a or SPCA2 WT *versus* the catalytic dead mutants shows that the TFE3-GFP translocation or Golgi stress are not merely consequences of the transfection procedure or overexpression of a Golgi protein. Instead, our data indicate that the induction of Golgi stress depends on SPCA1a activity, indicating that the increased $Ca^{2+}$ level in the non-ER stores is responsible.

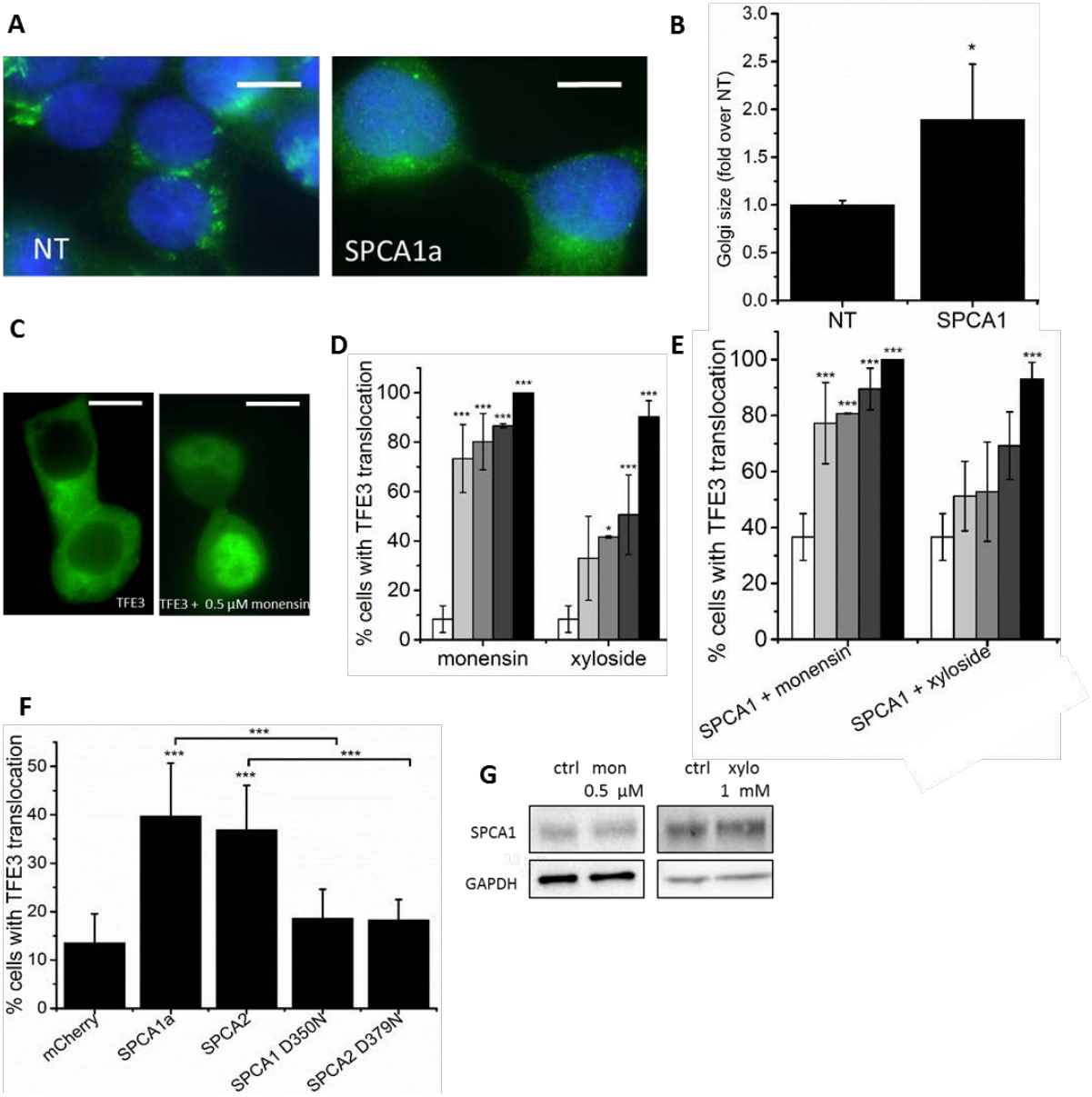


**Figure 3: SPCA1a overexpression results in Golgi stress.** A) The trans-Golgi network expands by the overexpression of SPCA1a. B) Quantification of Golgi size relative to the size of the nucleus, normalized to non-transfected (NT) cells. C) Treatment of HEK293T cells with monensin causes TFE3 translocation to the nucleus. D) and E) TFE3 translocation in HEK293T control cells (D) or cells transfected with SPCA1 with increasing concentrations of stress inducers. Monensin: 0; 0.5 µM; 1 µM; 2 µM; 5 µM. Xyloside: 0; 1 mM; 2 mM; 5 mM; 10 mM. F) TFE3-GFP translocation with overexpression of SPCA1a, SPCA2 or their inactive mutants. G) SPCA1a expression levels are unchanged after 48 h incubation with the Golgi stress inducers monensin (mon, 0.5 µM) and xyloside (xyl, 1 mM) *versus* control (ctrl). Values are represented as average ± SD. n=3. Scale bar: 10 µm. 100 cells were counted per condition, n=3. *:p<0.05; **: p<0.01; ***: p<0.005

The translocated TFE3 promotes expression of several Golgi related genes in the nucleus by binding to GASE stress recognition elements (consensus sequence ACGTGGC) and several putative GASE motifs are found in the promoter region of *ATP2C1* (Supplementary Table 1). However, treatment with monensin or xyloside did not increase the endogenous SPCA1 expression, indicating that induction of SPCA1 expression is not part of the Golgi stress response (Figure 3G).

In conclusion, the overexpression of SPCA1a or SPCA2 causes Golgi stress, which relates to elevated $Ca^{2+}$ uptake into the non-ER compartments.

*3.4 Several SPCA1a Hailey-Hailey disease mutants display a reduced capacity to activate Orai1*

Over 170 HHD-associated mutations have so far been identified in SPCA1, but not all of them impair SPCA1 activity [5, 7], suggesting that other SPCA1-related functions may be affected. We explored whether such HHD mutations may reduce the capacity of SPCA1a to activate Orai1. We selected two mutants that present normal autophosphorylation activity (P201L and I580V), one catalytically impaired mutant (G309C) [5], two truncation mutants (Q259X and R799X) and D644G, an uncharacterized HHD mutant [8] (Table 1). We followed a similar approach as for WT and expressed the HHD mutants as N-terminal mCherry fusion proteins in HEK293T cells. All mutants, except R799X, are expressed to a similar level as WT and apart from the truncation mutants, all disease mutants display a similar Golgi-like distribution (Supplementary Figure 2).

| Mutation | Number of reported cases of HHD[1] | Phosphorylation |
|---|---|---|
| **Wild-type** | | Yes |
| **P201L** | 2 | Yes |
| **Q259X** | 1 | No |
| **G309C** | 1 | No |
| **I580V** | 2 | Yes |
| **D644G** | 1 | No |
| **R799X** | 14 | No |

**Table 1: Overview of the selected HHD mutations.** [1]The reported number of HHD cases associated with each mutation is copied from [8].

We first compared the biochemical properties of the mutants by autophosphorylation (Figure 4A, Table 1) and ATPase experiments (Figure 4B) and then assessed their ability to induce $Ca^{2+}$ influx (Figure 4C). Several mutant classes are recognized. The two truncation mutants are catalytically inactive and display an impaired ability to activate Orai1. The point mutants G309C and D644G both fail to undergo autophosphorylation, but in contrast to D644G, only G309C retains a normal capacity to trigger $Ca^{2+}$ influx. Mutants P201L and I580V present normal autophosphorylation levels and display in ATPase experiments a similar apparent $Ca^{2+}$ affinity as WT SPCA1a, while the maximal turnover rates are slightly lower (P201L: 66% of WT, I580V: 83% of WT). However, in contrast to P201L, the I580V mutant evokes a weaker SICE response than WT SPCA1a. Irrespective of these differences, all mutants display a lower $Ca^{2+}$ content of the TG-insensitive stores as compared to WT (Figure 4D). Interestingly, the relative differences in the ionomycin-dependent $Ca^{2+}$ release reflect the combined SPCA1a and/or Orai1 activity (Figure 4A-C) and correlates well to the percentage of cells displaying TFE3-GFP

translocation (Figure 4E, Supplementary Figure 3). This confirms that the degree of TFE3-GFP translocation follows the $Ca^{2+}$ content of the TG-insensitive stores.

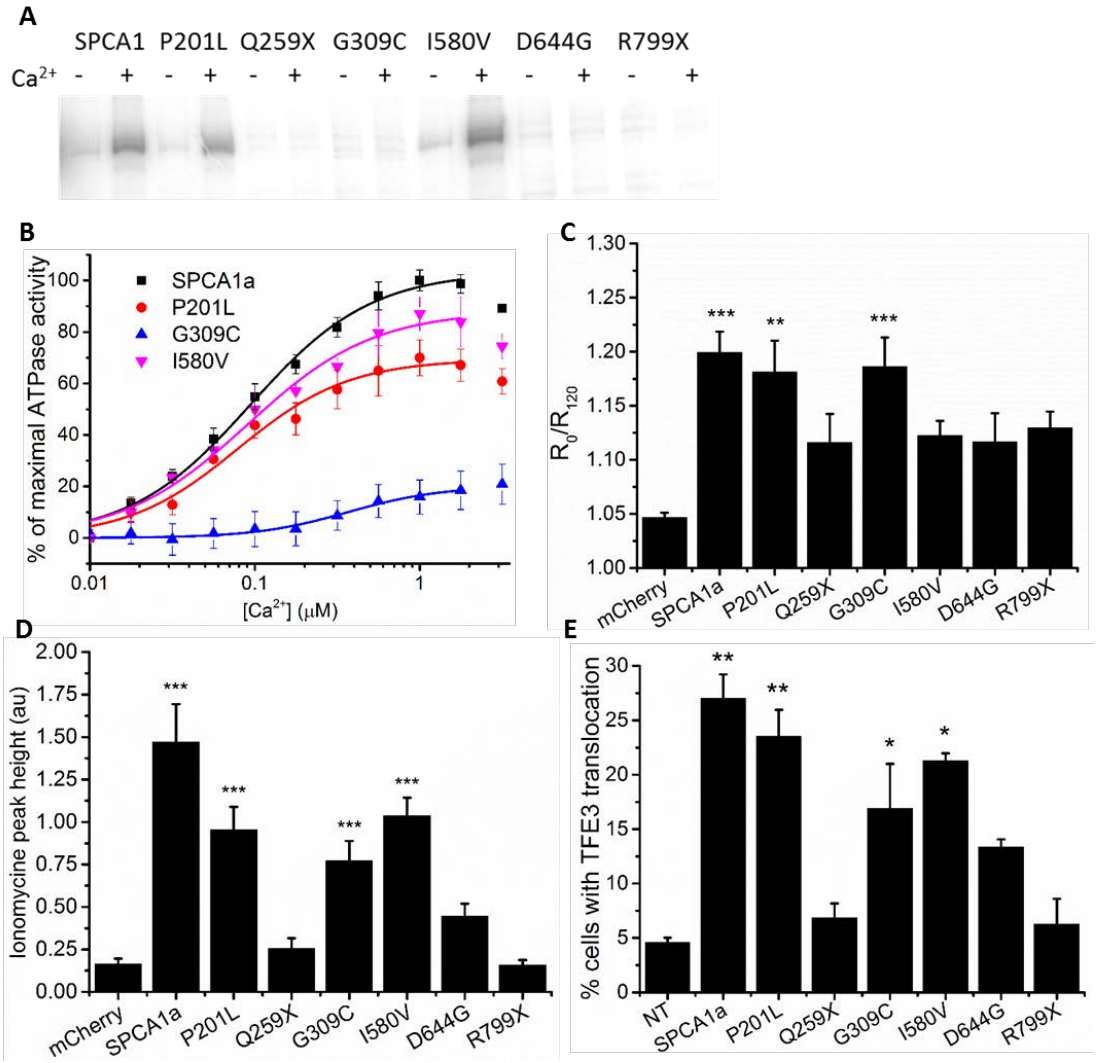


**Figure 4: Biochemical characterization of Hailey-Hailey disease (HHD) mutants.** A) $^{32}$P-ATP phosphorylation of the HHD mutants in the presence or absence of 1 µM $Ca^{2+}$. B) $Ca^{2+}$-dependent ATPase activity of WT SPCA1 and the HHD mutants P201L, G309C and I580V. C) Constitutive $Ca^{2+}$ influx induced by overexpression of HHD mutants. D) $Ca^{2+}$ release from TG-insensitive stores upon overexpression of HHD mutants, induced by ionomycine. E) TFE3-GFP translocation induced by overexpression of HHD mutants. Values are represented as average ± SEM. Fura-2: 10 cells per experiment were measured, n=4. TFE3-GFP translocation: 100 cells were counted per condition, n=3-6. *:p<0.05; **: p<0.01; ***: p<0.005

Thus, the investigated HHD mutants present an impaired SPCA1a activity, a reduced potential to activate Orai1 or both, which determines the intraluminal $Ca^{2+}$ concentration and the level of Golgi stress.

## 4. Discussion

In this study, we demonstrate that like SPCA2, SPCA1a is capable of activating Orai1, which increases the cytosolic $Ca^{2+}$ concentration. The $Ca^{2+}$ entering the cell is efficiently transferred into intracellular

compartments via SPCA1a-mediated $Ca^{2+}$ transport. An increased intraluminal $Ca^{2+}$ concentration correlates well with the induction of Golgi stress, highlighting for the first time the role of $Ca^{2+}$ into this organelle stress response. In our system, SPCA1-mediated SICE is probably initiated by the overexpression of SPCA1. While the physiological role of SPCA1-mediated SICE remains to be further established, our data indicate that the system may play a role in HHD, since several SPCA1 disease mutants display an impaired SICE response.

*4.1 Similarities and differences between SPCA1 versus SPCA2-mediated SICE*

We confirmed that the SPCA2-mediated rise in cytosolic $Ca^{2+}$ triggers NFAT translocation, while in the same expression system the rise in cytosolic $Ca^{2+}$ by SPCA1a-mediated SICE is insufficient to induce NFAT translocation [15, 16]. The inability of SPCA1a to induce NFAT translocation may relate to the slightly lower cytosolic $Ca^{2+}$ levels observed for SPCA1a in comparison to SPCA2, or may point to the involvement of specific microdomains.

The *ATP2C2* gene encoding SPCA2 appeared in vertebrate evolution before the rise of land life and originated from a gene duplication of the *ATP2C1* gene [3]. Since both SPCA1 and SPCA2 are capable of inducing SICE, it is likely that in evolution SPCA1 first developed the ability to activate Orai1, which may have been further specialized in SPCA2. In line with this hypothesis, both isoforms serve similar and partially overlapping functions in mammary gland cells. SPCA1 and SPCA2 are both upregulated during lactation and contribute to the $Ca^{2+}$ release into the milk [20]. However, it is likely that both SICE systems are regulated differently. The more restricted tissue distribution of SPCA2 expression indicates that the SPCA2-mediated SICE may be regulated mainly at the expression level [21]. The high SPCA2 expression in lactation and some forms of breast cancer induces SICE. The SPCA2-mediated system may be especially important for secretory cells that require high levels of $Ca^{2+}$ [15]. In contrast, SPCA1 is ubiquitously expressed, so it is likely that a molecular mechanism is in place to regulate SICE [21]. Continuous $Ca^{2+}$ influx would put the cells at risk for $Ca^{2+}$ overload, Golgi stress and even cell death.

Possible differences in the regulation of SICE may depend on sequence variations between the SPCA1 and SPCA2 N-terminus. In SPCA2, the N-terminus is responsible for binding to Orai1, allowing the C-terminus to come close enough to activate Orai1 [15]. It was shown that also the SPCA1 C-terminus retains the capacity to activate Orai1. However, in the presence of the SPCA1 N-terminus no Orai1 activation was observed [15]. In line with a major role for the N-terminus, we observed that SPCA1b and SPCA1d, which only differ from SPCA1a at the C-terminus, also induce SICE. The different regulation of SICE between SPCA1 and SPCA2 seems to depend on four amino acids in the N-terminus

that differ between SPCA1a and SPCA2 [15]. Noteworthy, an EF-hand like motif is found in the SPCA1 N-terminus at the corresponding SPCA2 site responsible for Orai1 binding. This suggests that a $Ca^{2+}$ sensor may control the activity of SPCA1 and/or Orai1, which will be further addressed in a separate study. One limitation of our current method is that the overexpression of SPCA1 or SPCA2 mCherry fusion proteins may overrule the endogenous regulation mechanism by the high expression levels or by the mCherry fusion, possibly explaining the constitutive activation of the system.

*4.2 Role of SPCA1a in Golgi stress*

SPCA1-mediated SICE may be part of the cellular response mechanism to Golgi stress, in analogy to the role of SOCE in ER stress. Upon $Ca^{2+}$ depletion in the ER, STIM1-mediated Orai1 activation leads to an increased cytosolic $Ca^{2+}$ concentration, which is then transferred into the ER by the SERCA2b pump, restoring the ER store content [22]. A similar mechanism may be in place in the Golgi and secretory pathway, where $Ca^{2+}$ levels could decline due to the expansion of the Golgi in conditions of Golgi stress, or when $Ca^{2+}$ is released during protein secretion. In SPCA1 knockout mice it was previously shown that the lack of SPCA1 leads to Golgi swelling and fragmentation during embryonic development, which are signs of Golgi stress [9, 23]. Our original hypothesis was therefore that low $Ca^{2+}$ levels in the Golgi may result in Golgi stress, which may then induce the SICE response. However, we show in our overexpression model that the induction of the Golgi stress marker TFE3 is strongly correlated with *higher* levels of $Ca^{2+}$ in the Golgi, which is related to the combined activation of SICE and SPCA1. This illustrates that high Golgi $Ca^{2+}$ levels induce Golgi stress. Unfortunately, in our overexpression system, we could not confirm nor exclude the possibility that SICE may be triggered as a response to lower $Ca^{2+}$ levels in the Golgi. This needs to be verified on endogenous SPCA1 and would require selective depletion of Golgi $Ca^{2+}$, which is difficult to achieve due to the lack of selective SPCA1 inhibitors. Until better tools for depleting Golgi $Ca^{2+}$ become available, the relationship between $Ca^{2+}$ and Golgi stress remains difficult to study.

So far, no $Ca^{2+}$-sensitive sensor proteins are known that are involved in the Golgi stress response or the activation of the SPCA1a/Orai1 system. In the trans-Golgi network, the luminal $Ca^{2+}$-binding protein Cab45 mediates the sorting of a subset of secretory proteins [24]. Cab45 colocalizes with SPCA1a and controls the $Ca^{2+}$ concentration of the TGN [4], suggesting that Cab45 may play a role in regulating luminal $Ca^{2+}$ levels in response to stress.

*4.3 Implications of SPCA1a-mediated activation of Orai1 in disease*

We tested a series of HHD mutants for their ATPase activity and ability to induce SICE in overexpression. We observed that all Hailey Hailey disease mutants are less capable of filling the TG-insensitive stores (Fig. 4D). However, we also show that several underlying molecular mechanisms can be responsible (Fig. 4A-C). We show that the ATPase activity of some HHD mutants is impaired, without affecting the capacity to induce SICE (G309C). Other mutants display a normal ATPase activity, but are clearly impaired in their ability to induce SICE (I580V). Of interest, mutants impaired in both the SPCA1 activity and SICE response display the lowest internal store $Ca^{2+}$ content. This suggests that loss of transport activity can be partially compensated by the ability to elicit SICE, provided that some functional SPCA pumps are present in the cell. This is generally the case in HHD, where only one of two copies of *ATP2C1* is affected. So far, we explored the effect of the disease mutants in an overexpression model, which represents a limitation, as it not accurately reflects the loss-of-function condition that is typically associated with HHD. Future studies in disease models will be required to further establish the role of SICE in HHD.

Besides HHD, SPCA1a and SPCA2 are upregulated in specific breast cancer sub-types. Higher levels of SPCA1 are found in basal-type breast tumors, whereas SPCA2 is upregulated in luminal-type tumors [15, 25]. $Ca^{2+}$ dyshomeostasis and high concentrations of cytosolic $Ca^{2+}$ are often found in cancer cells [26]. We show that SICE leads to increased $Ca^{2+}$ levels both in the cytosol and the lumen of non-ER stores [16], but the role of the cytosolic *versus* luminal $Ca^{2+}$ changes in pathological conditions remains to be further investigated. Upregulation of SPCA1 or SPCA2 may promote micro-calcifications in ductal carcinomas, which consist of precipitates of $Ca^{2+}$ phosphate or hydroxyapatite and are associated with a worse outcome [25].

In conclusion, we describe that the housekeeping isoform SPCA1, like SPCA2, can promote SICE. The physiological function and regulation of SPCA1-mediated Orai1 activation remains to be fully established, but the system may provide sufficient uptake of $Ca^{2+}$ in the lumen of the secretory pathway under specific cellular conditions or in specific cell types like secretory cells. In addition, the SPCA1/Orai1 system may be implicated in the Golgi stress pathway, since we establish a clear link between altered luminal $Ca^{2+}$ levels and the induction of Golgi stress. Finally, a dysregulated SPCA1/Orai1 system may contribute to the impaired $Ca^{2+}$ homeostasis in HHD.

**Acknowledgements**

We thank Dr. F. Wuytack and Dr. J. Vanoevelen for their input at the start of the project. This work was funded by the Flanders Research Foundation FWO (G044212N and G0B1115N) and the Inter-University Attraction Poles program (P7/13).

**Conflict of interest**

The authors declare that they have no conflicts of interest.

**Author contributions**

PV conceived and coordinated the study. SS performed experiments and analyzed the data. SS and PV wrote the manuscript. PV, JC and JE critically reviewed the manuscript. SK and TV provided assistance with TIRF microscopy. All authors reviewed the results and approved the final version of the manuscript.

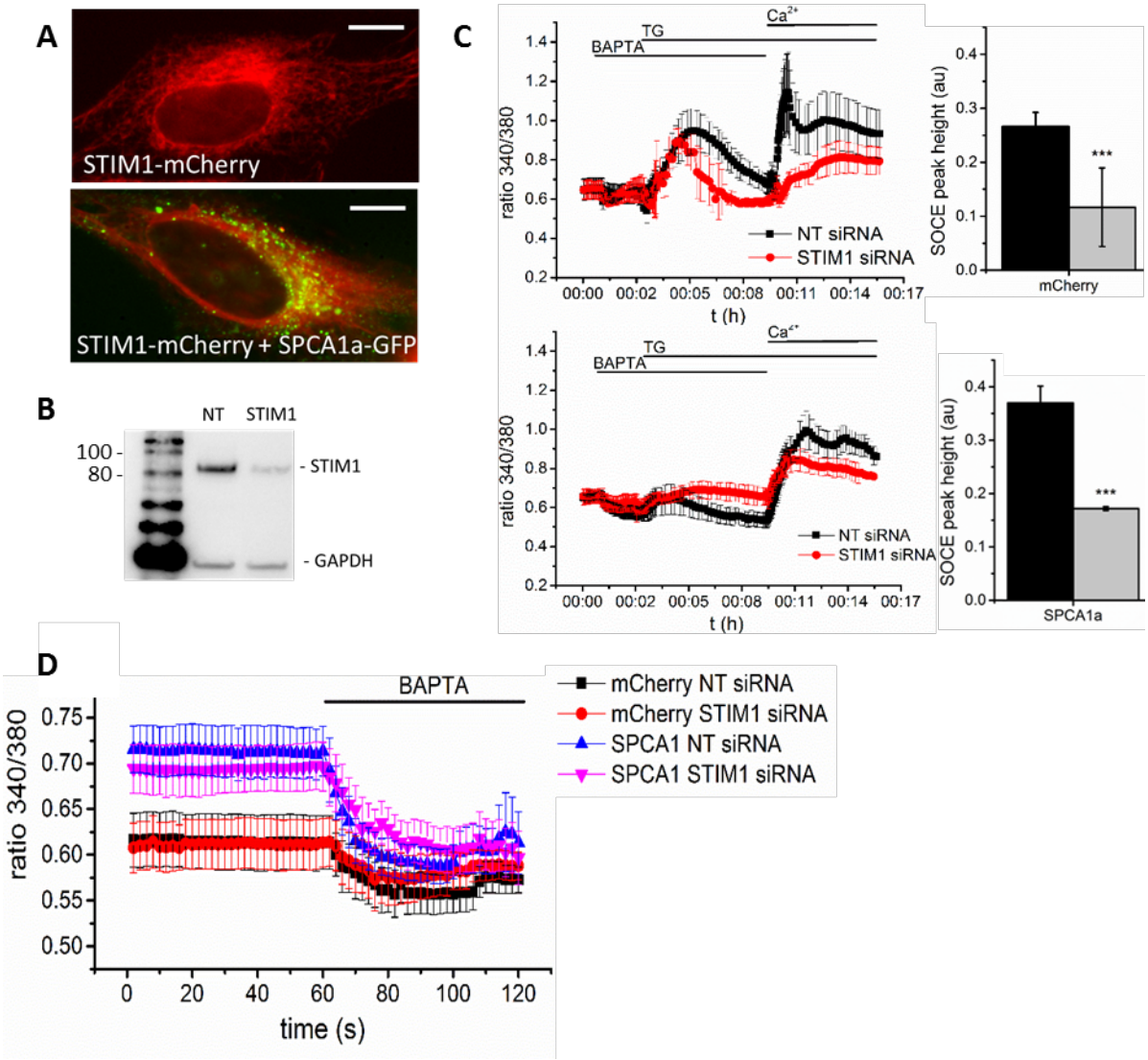


**Supplementary figure 1: SICE occurs independently of STIM1.** A) STIM1 cellular localization is unaltered with overexpression of SPCA1a in HeLa cells. B) Immunoblotting depicts that STIM1 protein expression is reduced by 65% with STIM1 siRNA compared to non-targeting (NT) siRNA. C) Following store depletion with TG, store-operated $Ca^{2+}$ entry is with STIM1 knockdown in cells with mCherry (top panel) or SPCA1a overexpression (bottom panel). Left panels: representative $Ca^{2+}$ traces; right panels: average SOCE response ± SEM (n = 3-4). 10 cells were measured per experiment. D) Store-independent $Ca^{2+}$ entry is unaltered upon STIM1 knockdown. Traces represent average of 4 experiments, 10 cells were measured per experiment.

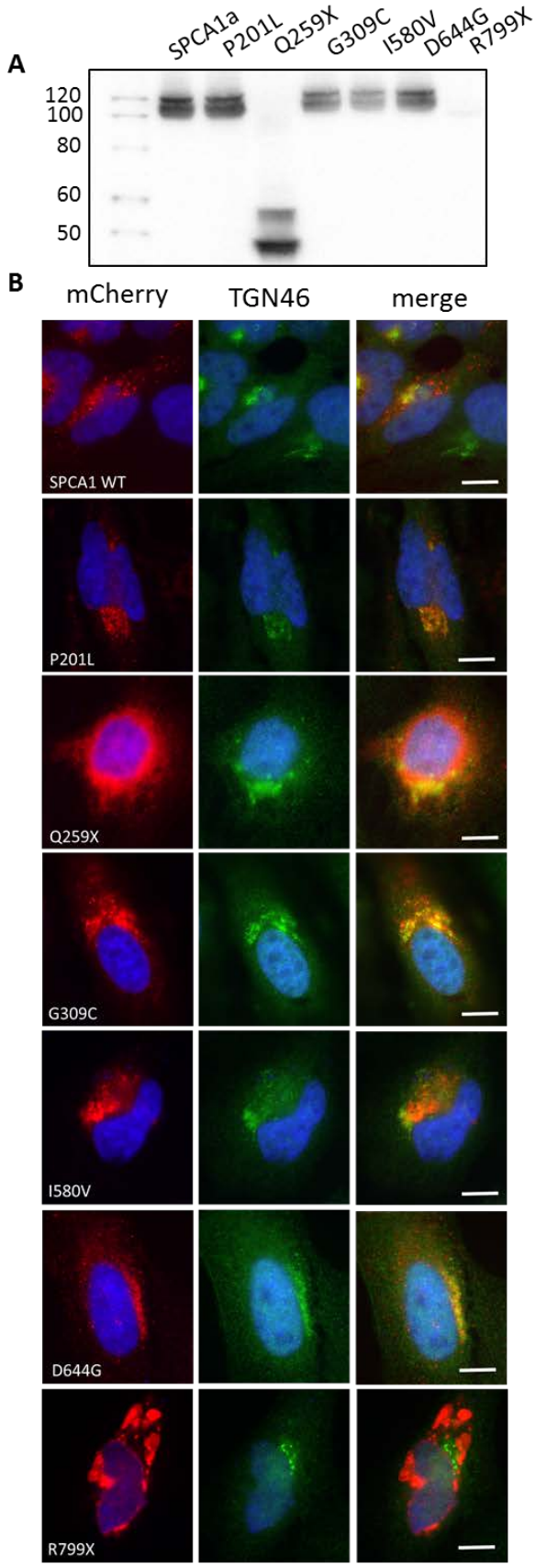


**Supplementary figure 2: Expression and localization of Hailey Hailey disease (HHD) mutants.** A) Immunoblot of mCherry-tagged HHD mutants upon overexpression in HEK293T cells. B) Co-localization of mCherry-tagged HHD mutants and TGN46 in HeLaT1 cells. Scale bar: 10 µm.

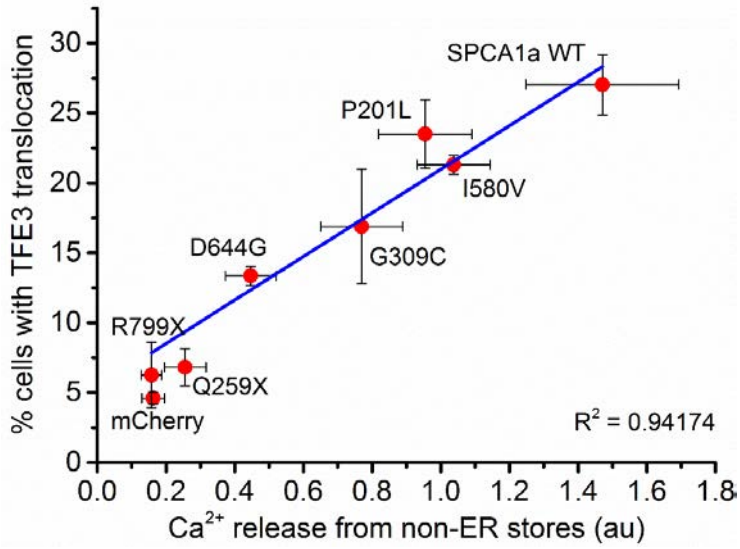


**Supplementary figure 3: Correlation between the $Ca^{2+}$ release from non-ER stores and TFE3 translocation for HHD mutants.** The ionomycin-induced $Ca^{2+}$ release after previous addition of TG (Figure 4D) was plotted against the % of cells with nuclear translocation of the Golgi stress marker TFE3 (Figure 4E).

| Gene | Sequence | Start position |
|---|---|---|
| *ATP2C1* | CCGTGGC | -57 |
| | GCGTGGC | -143 |
| | GCGTGGC | -1044 |

**Supplementary table 1: prevalence of GASE recognition sequence.** The consensus sequence is ACGTGGC, with variations allowed in the first or last base only.

**References**


1. Brini, M. and E. Carafoli, *Calcium pumps in health and disease.* Physiol Rev, 2009. **89**(4): p. 1341-78.
2. Durr, G., et al., *The medial-Golgi ion pump Pmr1 supplies the yeast secretory pathway with Ca2+ and Mn2+ required for glycosylation, sorting, and endoplasmic reticulum-associated protein degradation.* Mol Biol Cell, 1998. **9**(5): p. 1149-62.
3. Vangheluwe, P., et al., *Intracellular $Ca^{2+}$- and $Mn^{2+}$-transport ATPases.* Chem Rev, 2009. **109**(10): p. 4733-59.
4. Crevenna, A.H., et al., *Secretory cargo sorting by Ca2+-dependent Cab45 oligomerization at the trans-Golgi network.* J Cell Biol, 2016. **213**(3): p. 305-14.
5. Fairclough, R.J., et al., *Effect of Hailey-Hailey Disease mutations on the function of a new variant of human secretory pathway Ca2+/Mn2+-ATPase (hSPCA1).* J Biol Chem, 2003. **278**(27): p. 24721-30.
6. Sudbrak, R., et al., *Hailey-Hailey disease is caused by mutations in ATP2C1 encoding a novel $Ca^{2+}$ pump.* Hum Mol Genet, 2000. **9**(7): p. 1131-40.
7. Nellen, R.G., et al., *Mendelian Disorders of Cornification Caused by Defects in Intracellular Calcium Pumps: Mutation Update and Database for Variants in ATP2A2 and ATP2C1 Associated with Darier Disease and Hailey-Hailey Disease.* Hum Mutat, 2016. **38**(4): p. 343-56.
8. Micaroni, M., et al., *ATP2C1 gene mutations in Hailey-Hailey disease and possible roles of SPCA1 isoforms in membrane trafficking.* Cell Death Dis, 2016. **7**(6): p. e2259.
9. Okunade, G.W., et al., *Loss of the Atp2c1 secretory pathway $Ca^{2+}$-ATPase (SPCA1) in mice causes Golgi stress, apoptosis, and midgestational death in homozygous embryos and squamous cell tumors in adult heterozygotes.* J Biol Chem, 2007. **282**(36): p. 26517-27.
10. Krebs, J., L.B. Agellon, and M. Michalak, *Ca(2+) homeostasis and endoplasmic reticulum (ER) stress: An integrated view of calcium signaling.* Biochem Biophys Res Commun, 2015. **460**(1): p. 114-21.
11. Miyata, S., et al., *The endoplasmic reticulum-resident chaperone heat shock protein 47 protects the Golgi apparatus from the effects of O-glycosylation inhibition.* PLoS One, 2013. **8**(7): p. e69732.
12. Martina, J.A., et al., *The nutrient-responsive transcription factor TFE3 promotes autophagy, lysosomal biogenesis, and clearance of cellular debris.* Sci Signal, 2014. **7**(309): p. ra9.
13. Oku, M., et al., *Novel cis-acting element GASE regulates transcriptional induction by the Golgi stress response.* Cell Struct Funct, 2011. **36**(1): p. 1-12.
14. Taniguchi, M., et al., *TFE3 is a bHLH-ZIP-type transcription factor that regulates the mammalian Golgi stress response.* Cell Struct Funct, 2015. **40**(1): p. 13-30.
15. Feng, M., et al., *Store-independent activation of Orai1 by SPCA2 in mammary tumors.* Cell, 2010. **143**(1): p. 84-98.
16. Smaardijk, S., et al., *SPCA2 couples Ca2+ influx via Orai1 to Ca2+ uptake into the Golgi/secretory pathway.* Tissue Cell, 2017. **49**(2 Pt A): p. 141-149.
17. Ghosh, D., et al., *VAMP7 regulates constitutive membrane incorporation of the cold-activated channel TRPM8.* Nat Commun, 2016. **7**: p. 10489.
18. Holemans, T., et al., *Measuring Ca2+ pump activity in overexpression systems and cardiac muscle preparations.* Cold Spring Harb Protoc, 2014. **2014**(8): p. 876-86.
19. Dode, L., et al., *Dissection of the functional differences between human secretory pathway $Ca^{2+}/Mn^{2+}$-ATPase (SPCA) 1 and 2 isoenzymes by steady-state and transient kinetic analyses.* J Biol Chem, 2006. **281**(6): p. 3182-9.
20. Faddy, H.M., et al., *Localization of plasma membrane and secretory calcium pumps in the mammary gland.* Biochem Biophys Res Commun, 2008. **369**(3): p. 977-81.
21. Vanoevelen, J., et al., *The secretory pathway $Ca^{2+}/Mn^{2+}$-ATPase 2 is a Golgi-localized pump with high affinity for $Ca^{2+}$ ions.* J Biol Chem, 2005. **280**(24): p. 22800-8.

22. Liou, J., et al., *STIM is a Ca2+ sensor essential for Ca2+-store-depletion-triggered Ca2+ influx.* Curr Biol, 2005. **15**(13): p. 1235-41.
23. Lissandron, V., et al., *Unique characteristics of Ca2+ homeostasis of the trans-Golgi compartment.* Proc Natl Acad Sci U S A, 2010. **107**(20): p. 9198-203.
24. von Blume, J., et al., *Cab45 is required for Ca2+-dependent secretory cargo sorting at the trans-Golgi network.* J Cell Biol. , 2012. **199**(7): p. 1057-66.
25. Dang, D., H. Prasad, and R. Rao, *Secretory pathway Ca2+ -ATPases promote in vitro microcalcifications in breast cancer cells.* Mol Carcinog, 2017. **56**(11): p. 2474-2485.
26. Mignen, O., et al., *Constitutive calcium entry and cancer: updated views and insights.* Eur Biophys J, 2017. **46**(5): p. 395-413.